

# MICROBUNCHING INSTABILITY IN THE PRESENCE OF INTRABEAM SCATTERING FOR SINGLE-PASS ACCELERATORS\*

Cheng-Ying Tsai<sup>†</sup>, Huazhong University of Science and Technology, Wuhan, China  
Weilun Qin<sup>‡</sup>, Deutsches Elektronen-Synchrotron DESY, Hamburg, Germany

## Abstract

Intrabeam scattering (IBS) has long been studied in lepton or hadron storage rings as a slow diffusion process, while the effects of IBS on single-pass or recirculating electron accelerators have drawn attention only in the recent two decades due to the emergence of linac-based or ERL-based 4th-generation light sources, which require high-quality electron beams during the beam transport. Recent experimental measurements indicate that in some parameter regimes, IBS can have a significant influence on microbunched beam dynamics. Here we develop a theoretical formulation of microbunching instability (MBI) in the presence of IBS for single-pass accelerators. We start from the Vlasov-Fokker-Planck (VFP) equation, combining both collective longitudinal space charge and incoherent IBS effects. The linearized VFP equation with the corresponding coefficients is derived. The evolutions of the phase space density and energy modulations are formulated as a set of coupled integral equations. The formulation is then applied to a simplified single-pass transport line. The results from the semi-analytical calculation are compared and show good agreement with particle tracking simulations.

## INTRODUCTION AND MOTIVATION

The studies of incoherent single-particle and collective multi-particle effects are in general separated in accelerator beam dynamics in that the two dynamical phenomena usually involve different time scales. In this work the collective high-frequency (or short-range) effect is considered along with incoherent small-angle, multiple Coulomb scattering or intrabeam scattering (IBS) effect [1, 2]. Most of the existing analyses of MBI [3–7] assume the absence of incoherent effects. With incoherent effect, to the lowest order we would expect only a heating effect, increasing the intrinsic beam spread. When the increase in the beam spread is not enough, it can only mitigate MBI to a small extent. In case the beam is heated too much, the instability feedback loop for density-energy conversion is damped, and suppression of MBI may come at the cost of beam quality degradation (overheating). When the additional damping is just sufficient, it will lead to effective suppression of MBI.

From early analytical estimate [8] the IBS was not expected to play a significant role in linac-based FEL performance, especially when laser heater [9, 10] is installed.

The renewed interest of IBS in linac-based FEL can be due to realization of high-brightness electron guns that have progressed significantly in recent years. Table 1 illustrates the order of magnitude estimate about the IBS growth rate,  $\tau_{\text{IBS}}^{-1} \propto N/\gamma^2 \epsilon_x^N \epsilon_y^N \sigma_z \sigma_\delta$ , where  $N$  is the number of particles per bunch,  $\gamma$  the Lorentz relativistic factor,  $\epsilon_{x,y}^N$  the normalized transverse emittance,  $\sigma_z$  the bunch length, and  $\sigma_\delta$  the relative energy spread. It can be seen that the IBS growth rate for single-pass accelerator is two or three orders of magnitude larger than that of the storage ring. If a beam with a proper energy chirp passes through a bunch compressor section, the local bunch current can have large enhancement, e.g., a factor of 10 to 100 enhancement, and the IBS effect may become more evident. Although the electron beam in a single-pass accelerator may only travel at a distance of  $\sim 100$  m to  $\sim$ km, the aforementioned enhancement may lead to a small but visible effect on MBI. Therefore, an analysis of MBI in the presence of IBS shall have potential practical interest [11–14].

Table 1: Table of Parameters for Order of Magnitude Estimate on IBS Growth Rate

	Storage Ring Light Source	Middle-energy Single-pass Accelerator
Beam energy	$\sim$ GeV	$\sim 100$ MeV
Particles per bunch	$10^{10}$ or more	$10^8 \sim 10^9$
Peak current	50~100 A	100 ~ a few kA
Norm. emittances	$\sim \mu\text{m}$	1 $\mu\text{m}$ or lower
Energy spread	$10^{-3} \sim 10^{-4}$	$10^{-4}$ or smaller
Effective distance	$\infty$	100 m~a few km

## LINEAR MATRIX EQUATIONS

Due to the page limit, we will not summarize all the relevant formulas but only highlight a few important equations. The evolution of phase space density and energy modulations can be formulated in the linear, coupled integral equations, and expressed in the matrix form below [12, 13]

$$\begin{pmatrix} \mathcal{P} & \mathcal{Q} \\ \mathcal{R} & \mathcal{S} \end{pmatrix} \begin{bmatrix} \mathbf{b}_{k_z} \\ \mathbf{p}_{k_z} \end{bmatrix} = \begin{bmatrix} \mathbf{b}_0 \\ \mathbf{p}_0 \end{bmatrix}, \quad (1)$$

where  $\mathcal{P}, \mathcal{Q}, \mathcal{R}, \mathcal{S}$  includes the current-dependent effects, e.g., high-frequency impedance, phase space smearing, IBS-induced energy spread increase and emittance growth. Since  $\mathcal{P}, \mathcal{Q}, \mathcal{R}, \mathcal{S}$  are independent of  $\mathbf{b}_{k_z}, \mathbf{p}_{k_z}$ , the matrix equation can be solved analytically in a symbolic form; evaluation

\* This work was supported by the Fundamental Research Funds for the Central Universities under Project No. 5003131049 and the National Natural Science Foundation of China under Project No. 11905073.

<sup>†</sup> jcytsai@hust.edu.cn

<sup>‡</sup> weilun.qin@desy.de

of the matrices  $\mathcal{P}$ ,  $\mathcal{Q}$ ,  $\mathcal{R}$ ,  $\mathcal{S}$  and their inverses is straightforward.

## SLICE ENERGY SPREAD

An important figure of merit for FEL performance is the slice energy spread (SES). Following [11, 13, 14], we have the collective energy kick at the end of a beamline section

$$\Delta\delta_{s_f} \approx -2L_b C_{\text{tot}} \int_0^{s_f} \frac{d\lambda}{\lambda^2} \left[ \int_0^{s_f} d\tau \frac{I_b(\tau)}{\gamma I_A} Z_{\parallel}(\lambda; \tau) \tilde{G}(\lambda; \tau) \right] b(\lambda; 0), \quad (2)$$

where  $C_{\text{tot}} = C(s_f)$  and  $b(\lambda; 0)$  denotes the initial density modulation. The term  $C_{\text{tot}}$  pulled outside the  $\tau$  integration is based on the assumption that (if any) bunch compression occurs at  $s \approx s_f$ . This is a typical approximation as the length of a bunch compressor is usually much shorter than the straight section in a linear transport line. To estimate the increase of SES due to the collective effect, we take the mean square sum

$$\langle |\Delta\delta_{s_f}|^2 \rangle \leq 4L_b C_{\text{tot}} \int_0^{\lambda^*} \frac{d\lambda}{\lambda^2} \langle |b(\lambda; 0)|^2 \rangle \left| \int_0^{s_f} d\tau \frac{I_b(\tau)}{\gamma I_A} Z_{\parallel}(\lambda; \tau) \tilde{G}(\lambda; \tau) \right|^2, \quad (3)$$

where  $\lambda^* \approx \left| \frac{2\pi R_{56}^{\text{tot}}}{1-hR_{56}^{\text{tot}}} \right| \sigma_{\delta}$ . We remark that such  $\lambda^*$  roughly corresponds to the peak value of the integrand  $\left| \int_0^{s_f} d\tau Z_{\parallel}(\lambda; \tau) \tilde{G}(\lambda; \tau) \right|$ . The suppression (or phase space smearing) in microbunching gain factor  $\tilde{G}(\lambda; \tau)$ , which is proportional to  $\exp\left[-\frac{k_z^2}{2}(\dots)\right]$ , is only effective when the modulation wavelength is small enough (or  $k_z$  large enough). Those responsible for effective phase space smearing are attributed to the SES. An initial bunch density distribution consists of shot-noise fluctuations due to the discreteness or granularity of the elementary charge; thus the initial effective density modulation per unit length within a bandwidth can be written as  $\frac{d\lambda}{\lambda^2} \langle |b(\lambda; 0)|^2 \rangle = \frac{2e}{L_b I_b} \Delta f = \frac{2}{L_b n_b} \frac{d\lambda}{\lambda^2}$  with  $I_b = ec n_b$ . Thus we write the effective SES due to the collective interaction as

$$\sigma_{\delta, \text{coll}}^2 \approx \frac{8}{n_b} C_{\text{tot}} \int_0^{\lambda^*} \frac{d\lambda}{\lambda^2} \left| \int_0^{s_f} d\tau \frac{I_b(\tau)}{\gamma I_A} Z_{\parallel}(\lambda; \tau) \tilde{G}(\lambda; \tau) \right|^2. \quad (4)$$

A constant, numerical factor is introduced when benchmarking the semi-analytical calculation with particle tracking simulations. The overall SES in an electron beam can be attributed by the pure optics transport (e.g., bunch compression), by the incoherent IBS effect, and the collective effects. The total SES at  $s = s_f$  can be estimated by the quadrature sum of the individual contributions

$$\sigma_{\delta, \text{tot}} \approx \begin{cases} \sqrt{C_{\text{tot}}^2 \sigma_{\delta 0}^2 + C_{\text{tot}}^2 \sigma_{\delta, \text{coll}}^2}, & \text{without IBS} \\ \sqrt{\sigma_{\delta, \text{IBS}}^2 + C_{\text{tot}}^2 \sigma_{\delta, \text{coll}}^2}, & \text{with IBS} \end{cases} \quad (5)$$

with  $\sigma_{\delta 0}$  the initial SES.

## EXAMPLE: FODO-BC-FODO-BC TRANSPORT LINE

The schematic layout of this idealized model is shown in Fig. 1, where the two straight sections are composed of focusing-drift-defocusing-drift (FODO) magnetic elements. The two bunch compressors are identical, each made of four bending dipoles (with  $R_{56} \approx 48.9$  cm). Between the straight and chicane sections, additional quadrupole magnets are employed for beam optics matching. The beam energy is 150 MeV, peak current varying from 5 to 40 A depending on the initial chirp, the initial SES  $1.33 \times 10^{-5}$ ,  $\epsilon_{x,y}^N = 0.4 \mu\text{m}$ . For more details of the FODO design parameters, the reader is referred to Ref. [15]. The purpose of the two FODO sections is to retain the small transverse beam sizes to enhance IBS. For simplicity, we place the drift section between the focusing and defocusing quadrupoles; it can be replaced by an array of RF cavities for beam acceleration. The bunch compressor chicanes longitudinally compress an energy-chirped electron beam, enhance the bunch peak current, and thus augment the IBS effect. Throughout the beam transport, LSC is the most dominant and the only collective effect included in the following analysis. An amount of energy modulation that had been accumulated in the upstream straight sections would in part convert to the density modulation downstream through a nonzero longitudinal dispersion  $R_{56}$  and in the meanwhile contribute to the resultant SES.

It is interesting to observe from Fig. 1 that for low current case the total SES with IBS is *larger* than that without IBS throughout the beamline. In contrast, for the high current case the total SES with IBS becomes *lower* near the end of the beamline. Looking at the green dashed lines, we see that IBS plays a significant role to suppress MBI-induced SES. The semi-analytical calculations are in reasonable agreement with particle tracking simulations [16, 17]. Figures 2 and 3 further illustrate the SES along the bunch at the end of the beamline, indicating the effectiveness of IBS effects. When IBS-induced beam spread is not enough (e.g.,  $I_{b0} = 20$  A), it merely heats the beam. In case the beam is heated too much (e.g.,  $I_{b0} = 40$  A), suppression of MBI may come at the cost of beam quality degradation. When the additional damping is just about right, we have the threshold condition

$$C_{\text{tot}}^2 \sigma_{\delta 0}^2 + C_{\text{tot}}^2 \sigma_{\delta, \text{coll,wo/IBS}}^2 = \sigma_{\delta, \text{IBS}}^2 + C_{\text{tot}}^2 \sigma_{\delta, \text{coll,w/IBS}}^2, \quad (6)$$

which will lead to effective, optimal suppression of MBI. Together with the concept of MBI multi-stage amplification [18–20], one can simplify the integrand in Eq. (4) by a Gaussian and polynomial fit and obtain the equation for the threshold current  $I_{b0}^{\text{th}}$  with  $m = 2$  [13]

$$\Delta\sigma_{\delta, \text{IBS}}^2 \approx C_{\text{tot}}^2 \frac{8}{n_b} \Lambda^{2+2m} \sqrt{\frac{\pi}{2}} \sigma_* F_0 \left\{ 1 + \text{erf}\left(\frac{\lambda^*}{\sqrt{2}\sigma_*}\right) - \frac{e^{-B/\lambda^{*2}}}{\sqrt{D}} \left[ 1 + \text{erf}\left(\sqrt{D} \frac{\lambda^*}{\sqrt{2}\sigma_*}\right) \right] \right\}, \quad (7)$$

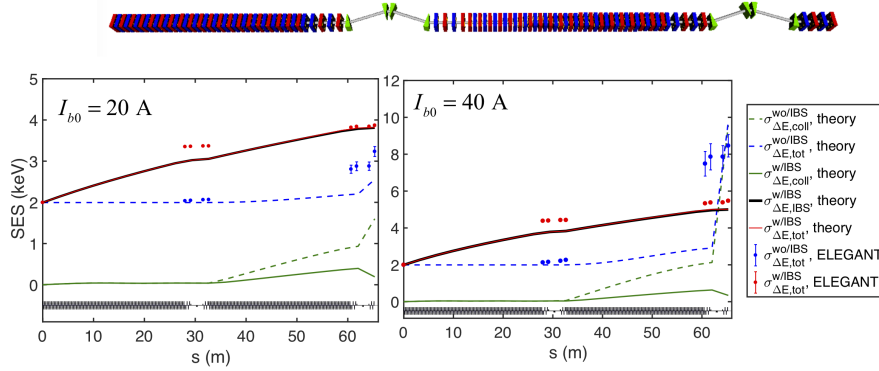


Figure 1: The schematic layout (top, not to scale) of the FODO-BC-FODO-BC transport line. The evolution of SES along  $s$  for  $I_{b0} = 20$  A (left) and  $I_{b0} = 40$  A (right) without bunch compression.

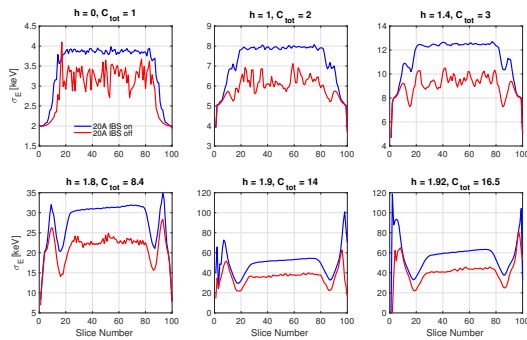


Figure 2: Final slice energy spread for  $I_{b0} = 20$  A for different energy chirps. In the simulation only LSC is included.

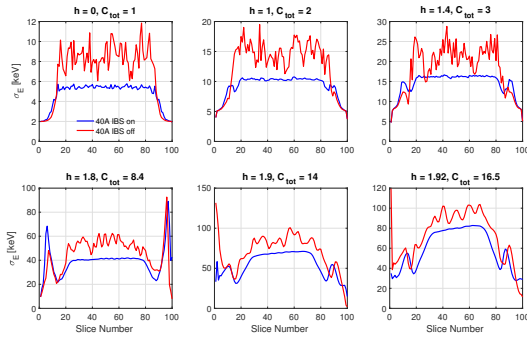


Figure 3: Final slice energy spread for  $I_{b0} = 40$  A for different energy chirps. In the simulation only LSC is included.

on the total bunch compression factor and the initial beam current. In this figure it can be observed that, for some fixed compression factor, the initial negative differences (i.e.,  $\sigma_{\Delta E, \text{tot}}^{\text{wo/IBS}} < \sigma_{\Delta E, \text{tot}}^{\text{w/IBS}}$ ) at low beam currents begin to change the sign (i.e.,  $\sigma_{\Delta E, \text{tot}}^{\text{wo/IBS}} > \sigma_{\Delta E, \text{tot}}^{\text{w/IBS}}$ ) as the beam current increases. This trend becomes even more evident for larger compression factors. For a fixed initial beam current, an increase of the compression factor means a larger beam current in the second FODO-BC section, thus enhancing both MBI and IBS. The interested reader is referred to Ref. [13] for more detailed discussion. Finally we remark that a similar analysis aiming for plasma-based accelerator FELs will be presented in this conference [21].

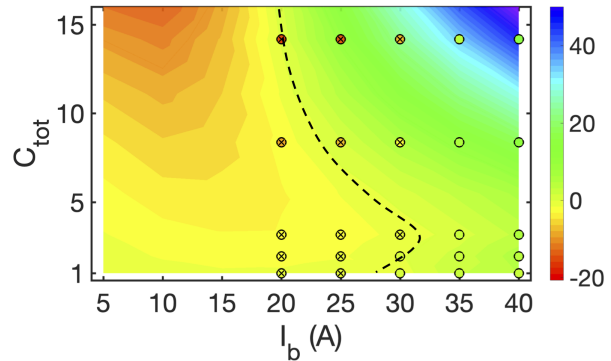


Figure 4:  $\circ$  and  $\otimes$  are elegant tracking. Background are results from VFP calculation. Dashed line refers to the case  $\sigma_{\Delta E, \text{tot}}^{\text{wo/IBS}} = \sigma_{\Delta E, \text{tot}}^{\text{w/IBS}}$ .

with  $\Lambda = I_b / \gamma I_A$ ,  $F_0$  and  $\sigma_*$  the fitting coefficients [13]

$$B = \frac{2\pi^2 R_{56, \text{tot}}^2 C_{\text{tot}}^4 r_e^2 I_{b0}}{\sqrt{2 \ln 2} e c \langle \sigma_x \rangle \epsilon_x^N \gamma^2} \left[ (s_1 - s_0) + \frac{1}{C_{\text{BC1}}} (s_f - s_1) \right], \quad (8)$$

where  $D = 1 + \frac{6B\sigma_*^2}{\lambda^{*4}}$ . Notice that  $I_{b0}$  is hidden in  $B$  and  $D$ .

Figure 4 shows the dependence of the resultant difference of SES without and with IBS, i.e.,  $\sigma_{\Delta E, \text{tot}}^{\text{wo/IBS}} - \sigma_{\Delta E, \text{tot}}^{\text{w/IBS}}$

## REFERENCES

- [1] A. Piwinski, "Intra-beam scattering", in *Proc. of the 9th Int. Conf. on High Energy Accelerators*, Stanford, CA, USA, p. 405. doi:10.5170/CERN-1992-001.226
- [2] K. Kubo, S. K. Mtingwa, and A. Wolski, "Intrabeam scattering formulas for high energy beams", *Phys. Rev. Accel. Beams*, vol. 8, p. 081001, 2005. doi:10.1103/PhysRevSTAB.8.081001

- [3] S. Heifets, G. Stupakov, and S. Krinsky, “Coherent synchrotron radiation instability in a bunch compressor”, *Phys. Rev. Accel. Beams*, vol. 5, p. 064401, 2002. doi:10.1103/PhysRevSTAB.5.064401
- [4] Z. Huang and K.-J. Kim, “Formulas for coherent synchrotron radiation microbunching in a bunch compressor chicane”, *Phys. Rev. Accel. Beams*, vol. 5, p. 074401, 2002. doi:10.1103/PhysRevSTAB.5.074401
- [5] M. Venturini, “Microbunching instability in single-pass systems using a direct two-dimensional Vlasov solver”, *Phys. Rev. Accel. Beams*, vol. 10, p. 104401, 2007. doi:10.1103/PhysRevSTAB.10.104401
- [6] C.-Y. Tsai, D. Douglas, R. Li, and C. Tennant, “Linear microbunching analysis for recirculation machines”, *Phys. Rev. Accel. Beams*, vol. 19, p. 114401, 2016. doi:10.1103/PhysRevAccelBeams.19.114401
- [7] C.-Y. Tsai, Ya. S. Derbenev, D. Douglas, R. Li, and C. Tennant, “Vlasov analysis of microbunching instability for magnetized beams”, *Phys. Rev. Accel. Beams*, vol. 20, p. 054401, 2017. doi:10.1103/PhysRevAccelBeams.20.054401
- [8] Z. Huang, “Intrabeam scattering in an x-ray FEL driver”, Stanford Linear Accelerator Center (SLAC), Menlo, Park, CA, USA, Rep. SLAC-TN-05-026, Nov. 2002.
- [9] E. L. Saldin, E. A. Schneidmiller, and M. V. Yurkov, “Klystron instability of a relativistic electron beam in a bunch compressor”, *Nucl. Instrum. Methods Phys. Res., Sect. A*, vol. 490, p. 1, 2002. doi:10.1016/S0168-9002(02)00905-1
- [10] Z. Huang *et al.*, “Suppression of microbunching instability in the linac coherent light source”, *Phys. Rev. ST Accel. Beams*, vol. 7, p. 074401, 2004. doi:10.1103/PhysRevSTAB.7.074401
- [11] S. Di Mitri *et al.*, “Experimental evidence of intrabeam scattering in a free-electron laser driver”, *New J. Phys.*, vol. 22, p. 083053, 2020. doi:10.1088/1367-2630/aba572
- [12] C.-Y. Tsai *et al.*, “Theoretical formulation of phase space microbunching instability in the presence of intrabeam scattering for single-pass or recirculation accelerators”, *Phys. Rev. Accel. Beams*, vol. 23, p. 124401, 2020. doi:10.1103/PhysRevAccelBeams.23.124401
- [13] C.-Y. Tsai and W. Qin, “Semi-analytical analysis of high-brightness microbunched beam dynamics with collective and intrabeam scattering effects”, *Phys. Plasma*, vol. 28, p. 013112, 2021. doi:10.1063/5.0038246
- [14] G. Perosa and S. Di Mitri, “Matrix model for collective phenomena in electron beam’s longitudinal phase space”, *Sci. Rep.*, vol. 11, p. 7895, 2021. doi:10.1038/s41598-021-87041-0
- [15] S. Di Mitri, “Intrabeam scattering in high brightness electron linacs”, *Phys. Rev. Spec. Top. Accel. Beams*, vol. 17, p. 074401, 2014. doi:10.1103/PhysRevSTAB.17.074401
- [16] M. Borland, “Elegant: A flexible SDDS-compliant code for accelerator simulation”, Argonne National Laboratory, Illinois, USA, Rep. LS-287, 2000.
- [17] Y. Wang and M. Borland, “Pelegant: A parallel accelerator simulation code for electron generation and tracking”, in *AIP Conf. Proc.*, Lake Geneva, Wisconsin USA, Jul. 2006, pp. 241–247. doi:10.1063/1.2409141
- [18] C.-Y. Tsai, “An alternative view of coherent synchrotron radiation induced microbunching development in multibend recirculation arcs”, *Nucl. Instrum. Methods Phys. Res. Sect. A*, vol. 943, p. 162499, 2019. doi:10.1016/j.nima.2019.162499
- [19] C.-Y. Tsai, “Concatenated analyses of phase space microbunching in high brightness electron beam transport”, *Nucl. Instrum. Methods Phys. Res. Sect. A*, vol. 940, pp. 462–474, 2019. doi:10.1016/j.nima.2019.06.061
- [20] C.-Y. Tsai, D. Douglas, R. Li, and C. Tennant, “Multistage CSR Microbunching Gain Development in Transport or Recirculation Arcs”, in *Proc. 37th Int. Free Electron Laser Conf. (FEL’15)*, Daejeon, Korea, Aug. 2015, pp. 263–268. doi:10.18429/JACoW-FEL2015-MOP087
- [21] G. Perosa and S. Di Mitri, “Modelling and Counteracting Microbunching Instability in Spreader Lines of Radiofrequency and Plasma-Based Accelerators for Free-Electron Lasers”, presented at the 12th Int. Particle Accelerator Conf. (IPAC’21), Campinas, Brazil, May 2021, paper WEPAB228, this conference.